BIOCHEMISTRY
including biophysical chemistry & molecular biology

Article

pubs.acs.org/biochemistry

Discovery of an L-Fucono-1,5-lactonase from cog3618 of the Amidohydrolase Superfamily

Merlin Eric Hobbs,[†] Matthew Vetting,[§] Howard J. Williams,[‡] Tamari Narindoshvili,[‡] Devon M. Kebodeaux,[‡] Brandan Hillerich,[§] Ronald D. Seidel,[§] Steven C. Almo,*[,§] and Frank M. Raushel*[,†,‡]

[†]Department of Biochemistry and Biophysics, Texas A&M University, College Station, Texas 77843, United States

[‡]Department of Chemistry, Texas A&M University, College Station, Texas 77843, United States

[§]Department of Biochemistry, Albert Einstein College of Medicine, 1300 Morris Park Avenue, Bronx, New York 10461, United States

Supporting Information

ABSTRACT: A member of the amidohydrolase superfamily, BmulJ_04915 from *Burkholderia multivorans*, of unknown function was determined to hydrolyze a series of sugar lactones: L-fucono-1,4-lactone, D-arabino-1,4-lactone, L-xylono-1,4-lactone, D-lyxono-1,4-lactone, and L-galactono-1,4-lactone. The highest activity was shown for L-fucono-1,4-lactone with a k_{cat} value of 140 s^{-1} and a k_{cat}/K_m value of 1.0×10^5 M^{-1} s^{-1} at pH 8.3. The enzymatic product of an adjacent L-fucose dehydrogenase, BmulJ_04919, was shown to be L-fucono-1,5-lactone via nuclear magnetic resonance spectroscopy. L-Fucono-1,5-lactone is unstable and rapidly converts non-enzymatically to L-fucono-1,4-lactone. Because of the chemical instability of L-fucono-1,5-lactone, 4-deoxy-L-fucono-1,5-lactone was enzymatically synthesized from 4-deoxy-L-fucose using L-fucose dehydrogenase. BmulJ_04915 hydrolyzed 4-deoxy-L-fucono-1,5-lactone with a k_{cat} value of 990 s^{-1} and a k_{cat}/K_m value of 8.0×10^6 M^{-1} s^{-1} at pH 7.1. The protein does not require divalent cations in the active site for catalytic activity. BmulJ_04915 is the second enzyme from cog3618 of the amidohydrolase superfamily that does not require a divalent metal for catalytic activity. BmulJ_04915 is the first enzyme that has been shown to catalyze the hydrolysis of either L-fucono-1,4-lactone or L-fucono-1,5-lactone. The structures of the fuconolactonase and the fucose dehydrogenase were determined by X-ray diffraction methods.

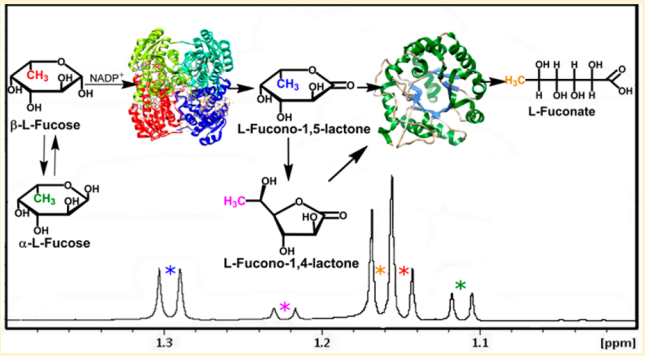

L-Fucose is a widely distributed monosaccharide throughout the biosphere having functions in both plant and mammalian glycoconjugates.[1,2] These glycoconjugates include the ABO blood group antigens in mammals, L-fucose binding lectins, glycolipids, and L-fucopyranosyl moieties in cell walls.[1] L-Fucose can function as the sole carbon source for many microbes and has been shown to be metabolized via two separate pathways as illustrated in Figure 1.[2−4] In the first pathway, L-fucose is isomerized to L-fuculose and then phosphorylated to L-fuculose 1-phosphate. It is subsequently cleaved to L-lactaldehyde and dihydroxyacetone phosphate.[3] In an alternative pathway, L-fucose is oxidized to L-fuconolactone and then hydrolyzed to L-fuconate. This product is subsequently dehydrated to 2-keto-3-deoxy-L-fuconate and then oxidized to 2,4-diketo-3-deoxy-L-fuconate. This compound is then hydrolyzed to pyruvate and L-lactate.[2] In the latter pathway, the enzymes that hydrolyze L-fuconolactone and 2,4-diketo-3-deoxy-L-fuconate have not been characterized.

We have determined the three-dimensional structure and functionally annotated BmulJ_04915 from *Burkholderia multivorans* ATCC 17616. Two homologues of this enzyme, Bamb_1224 from *Burkholderia ambifaria* AMMD and Patl_0798 from *Pseudoalteromonas atlantica* T6c, were also functionally annotated. These enzymes are members of the amidohydrolase superfamily (AHS) of enzymes from cog3618. Enzymes from this superfamily catalyze a diverse set of reactions, including the hydrolysis of amide or ester bonds, deamination, decarboxylation, isomerization, and hydration.[5] The structural hallmark for members of this superfamily is a distorted $(\beta/\alpha)_8$ barrel, which binds zero to three divalent metal ions within the active site.[5] The AHS has been separated into 24 clusters of orthologous groups (COG) by NCBI.[6]

The functionally characterized enzymes from cog3618 include 2-pyrone-4,6-dicarboxylate lactonase (LigI), 4-sulfomuconolactonase (4-SML), and L-rhamnono-1,4-lactonase.[7−9] A sequence similarity network for cog3618 at an *E* value cutoff of 10^{-30} is presented in Figure 2A.[10] In this figure, each node in the network represents a protein and is connected to other

Received: November 19, 2012
Revised: December 6, 2012
Published: December 10, 2012

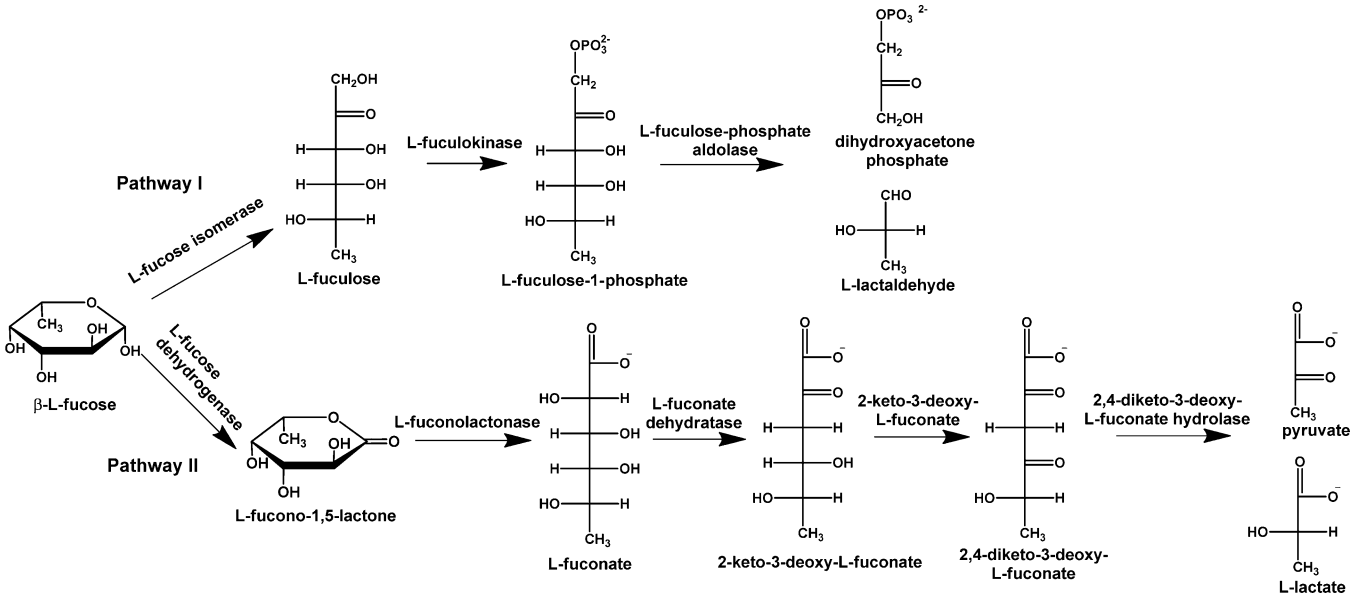

Figure 1. Metabolism of L-fucose. Pathway I produces dihydroxyacetone phosphate and L-lactaldehyde. Pathway II produces pyruvate and L-lactate through the oxidation of L-fucose to L-fucono-1,5-lactone.

proteins by edges when the BLAST *E* values are smaller than 10^{-30}. At this stringency, the proteins within cog3618 split into two large groups that are arbitrarily designated here as Class I and Class II. When a more stringent *E* value of 10^{-70} is applied to the sequence similarity network, the proteins organize into smaller groups (Figure 2B), which, because of their higher level of sequence similarity, may be isofunctional. In Figure 2, the groups are assigned an arbitrary numerical identifier (i.e., 1, 2, 3, etc.). L-Rhamnono-1,4-lactonase and BmulJ_04915 map to Class I, while LigI and 4-SML map to Class II. Genomic context analysis of the enzymes within Class I identifies many proteins of unknown function that are physically located near other genes that have been previously annotated as ABC-type carbohydrate transport systems, dehydrogenases, dehydratases, and hydrolases. Therefore, many of the proteins of unknown function within Class I are likely involved in carbohydrate metabolism and are thus predicted to hydrolyze sugar lactones.

BmulJ_04915 is predicted to hydrolyze sugar lactones based on genomic context (Figure 3). The protein, BmulJ_04922, from cog1028 is 64% similar in amino acid sequence to 2-keto-3-deoxy-L-fuconate dehydrogenase (XCC4067) from *Xanthomonas campestris*. BmulJ_04920 is 60% similar in protein sequence to the known L-fuconate dehydratase from cog4948 (XCC4069).[11,33] However, BmulJ_04919 from cog1028 is not related to XCC4067, an enzyme that is known to catalyze the oxidation of L-fucose. The closest experimentally annotated homologue to BmulJ_04919 is L-rhamnose dehydrogenase (SKA58_03570) from *Sphingomonas* sp. SKA58.[9] In this paper, we have determined the three-dimensional structures of BmulJ_04915 and BmulJ_04919 and have shown that BmulJ_04919 catalyzes the oxidation of L-fucose to L-fucono-1,5-lactone and that BmulJ_04915 and two homologues (Bamb_1224 and Patl_0789) catalyze the hydrolysis of this product to L-fuconate.

MATERIALS AND METHODS

Materials. All chemicals and buffers were purchased from Sigma Aldrich unless otherwise specified. Sugar lactones that were not commercially available were synthesized according to published procedures with the exception of 4-deoxy-L-fucono-1,5-lactone, which was enzymatically synthesized.[12] The noncommercial lactones included the following: L-fucono-1,4-lactone (**1**), D-altrono-1,4-lactone (**3**), D-arabinono-1,4-lactone (**6**), L-xylono-1,4-lactone (**7**), L-mannono-1,4-lactone (**11**), D-talono-1,4-lactone (**12**), D-allono-1,4-lactone (**13**), L-rhamnono-1,4-lactone (**14**), D-lyxono-1,4-lactone (**15**), L-lyxono-1,4-lactone (**16**), L-arabinono-1,4-lactone (**17**), D-xylono-1,4-lactone (**19**), L-mannono-1,5-lactone (**22**), L-rhamnono-1,5-lactone (**23**), and 4-deoxy-L-fucono-1,5-lactone (**24**). Those sugar lactones that were available commercially included the following: L-galactono-1,4-lactone (**2**), L-glucono-1,4-lactone (**4**), D-idono-1,4-lactone (**5**), D-mannono-1,4-lactone (**8**), D-glucono-1,4-lactone (**9**), D-galactono-1,4-lactone (**10**), D-ribono-1,4-lactone (**18**), D-glucurono-6,3-lactone (**20**), and D-erythronolactone (**21**). These compounds were obtained from CarboSynth or ChromaDex. The structures of these lactones are presented in Scheme 1. The aldose sugars were obtained from either from Sigma Aldrich or Carbosynth, and the structures are presented in Scheme 2. These sugars included L-fucose (**25**), L-galactose (**26**), L-glucose (**27**), D-altrose (**28**), D-arabinose (**29**), L-xylose (**30**), L-rhamnose (**31**), D-mannose (**32**), L-allose (**33**), D-talose (**34**), L-talose (**35**), D-allose (**36**), D-galactose (**37**), L-mannose (**38**), D-gulose (**39**), D-glucose (**40**), L-arabinose (**41**), L-ribose (**42**), D-lyxose (**43**), L-lyxose (**44**), D-xylose (**45**), D-ribose (**46**), and 4-deoxy-L-fucose (**47**).

Cloning, Expression, and Purification of BmulJ_04915 from *B. multivorans* ATCC 17616 and Patl_0798 from *P. atlantica* T6c. The gene for BmulJ_04915 (gil161520151) was amplified from *B. multivorans* ATCC 17616 genomic DNA using 5′-TTAAGAAGGAGATATACCATGGGTGCCCTGCGTATTGACTCAC-3′ as the forward primer and 5′-GATTGGAAGTAGAGGTTCTCTGCCAGACGAGCATCAGCCGGTTC-3′ as the reverse primer. The gene Patl_0798 (gil 109897125) was amplified from *P. atlantica* strain T6c genomic DNA using 5′-TTAAGAAGGAGATATACCATGGTGATGAGAATTGATGCACACCAACATT-3′ as the forward primer and 5′-GATTGGAAGTAGAGGTTCTCTGCCAATCGGTAGAATCGTTCGGC-3′ as the reverse primer. Polymerase

dx.doi.org/10.1021/bi3015554 | *Biochemistry* 2013, 52, 239−253

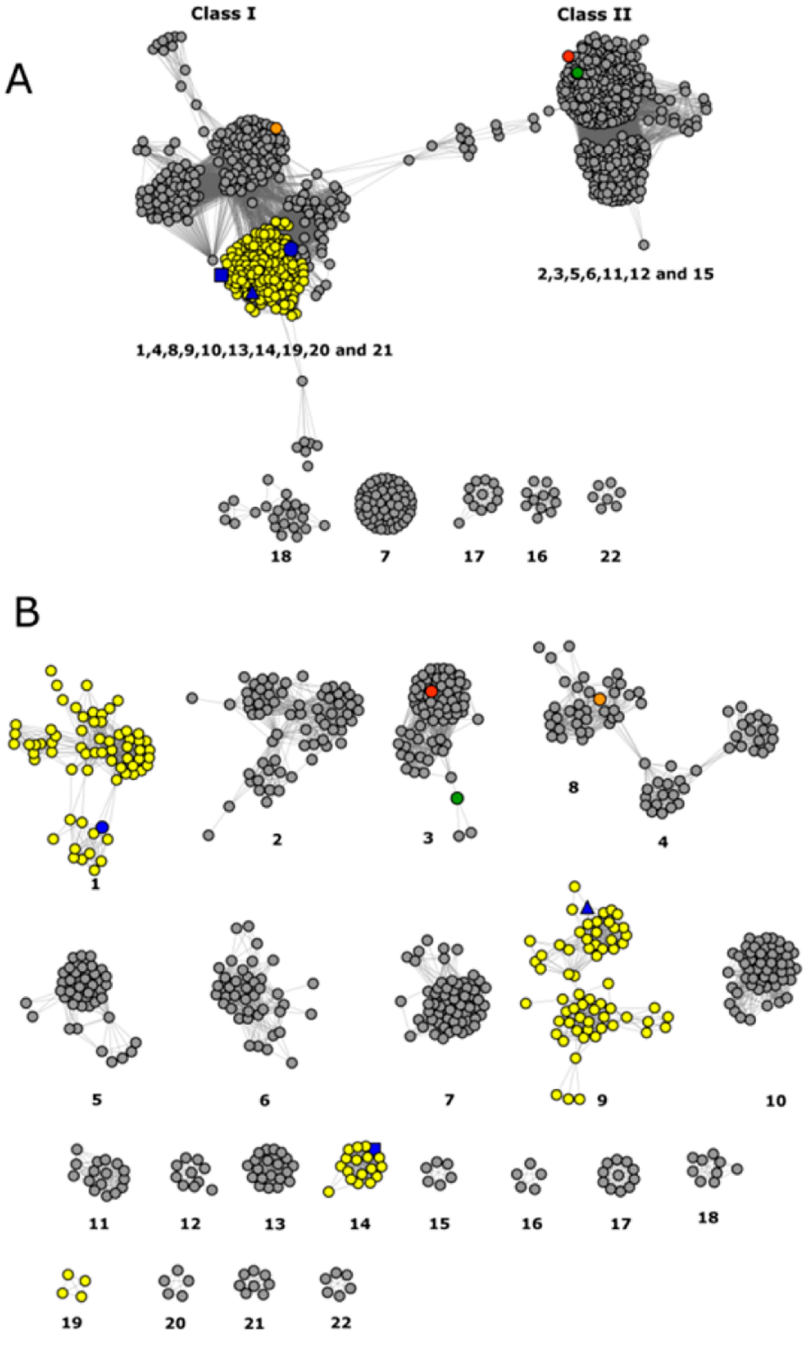

Figure 2. (A) cog3618 sequence similarity networks at an *E* value of 10^{-30} where each node represents a protein and an edge represents an *E* value between two proteins of $\leq 10^{-30}$. (B) cog3618 sequence similarity networks at an *E* value of 10^{-70} where each node represents a protein and an edge represents an *E* value between two proteins of $\leq 10^{-70}$. The nodes are color-coded as follows: yellow nodes for predicted L-fucono-1,5-lactonase, blue square for BmulJ_04915, blue circle for Bamb_1224, blue triangle for Patl_0798, orange node for L-rhamnono-1,4-lactonase, red node for LigI, and green node for Protein Data Bank entry 4SML.

chain reaction (PCR) was performed using KOD Hot Start DNA Polymerase (Novagen). The conditions were as follows: 2 min at 95 °C, followed by 40 cycles of 30 s at 95 °C, 30 s at 66 °C, and 30 s at 72 °C. The amplified fragments were cloned into the C-terminal TEV cleavable StrepII-6x-His-tag containing vector, CHS30, by ligation-independent cloning.[13]

All purification steps were performed at 4 °C, and all growth media contained 100 μg/mL kanamycin and 35 μg/mL chloramphenicol. The plasmid was transformed into Rosetta2-(DE3)pLysS cells (Novagen) and plated on LB agar plates. Five to ten colonies were used to inoculate 100 mL of LB medium and allowed to grow overnight at 37 °C (250 rpm agitation). The overnight cultures were used to inoculate 4 L of autoinduction medium in ten 2 L flasks and incubated (250 rpm agitation) at 25 °C for 24 h until the OD_{600} reached 20–25.[14,15] Cells were harvested by centrifugation and stored at −80 °C. Cells were resuspended (4:1, v/w) in buffer A [50 mM HEPES (pH 7.8), 150 mM NaCl, 10% glycerol, and 20 mM imidazole] with 0.1% Tween 20 and then disrupted by sonication. The cellular extract was clarified by centrifugation at 4 °C and applied to a 10 mL Ni-Sepharose HP (GE Healthcare) column. The column was washed with 10 column

dx.doi.org/10.1021/bi3015554 | *Biochemistry* 2013, 52, 239−253

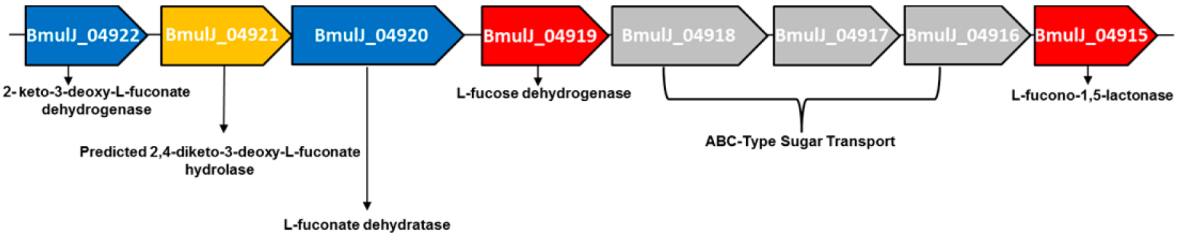

Figure 3. Genomic neighborhood of BmulJ_04915. Genes are color-coded as follows: red for those cloned and purified for this study, blue for those predicted from strong sequence similarity to genes encoding proteins of known function, yellow for those predicted genes based on genomic context, and gray for those predicted to function in carbohydrate transport.

Scheme 1

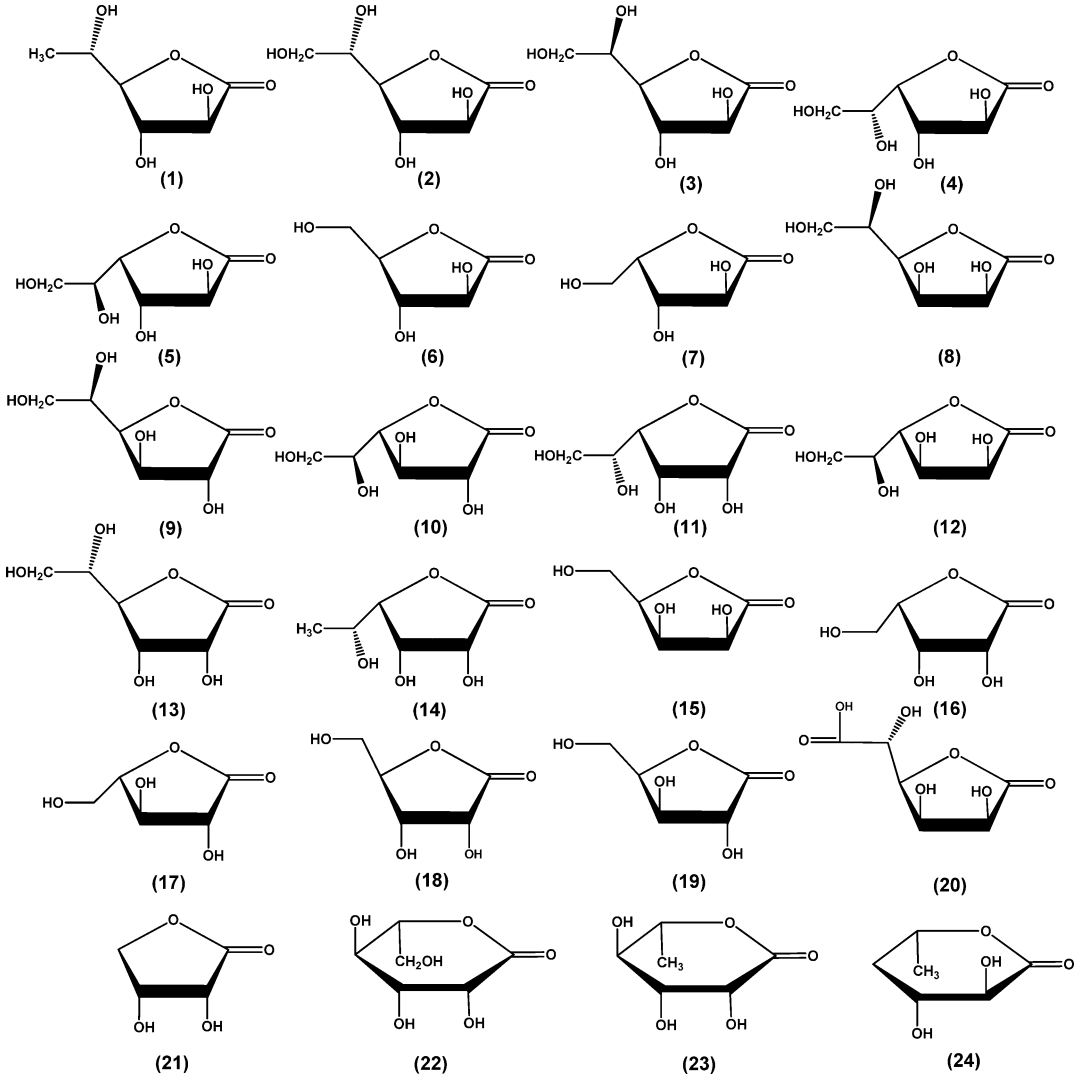

volumes of buffer A, and proteins were step eluted with 300 mM imidazole in buffer A. TEV protease[16] was added at a ratio of 1:50 (w/w) to the pooled fractions that were subsequently dialyzed overnight against buffer A with 300 mM imidazole. The pooled eluate was then concentrated to 15−30 mg/mL and applied to a 16/60 Superdex 200 column (GE Healthcare) equilibrated against buffer B [20 mM HEPES (pH 7.8), 150 mM NaCl, and 5% glycerol]. Fractions that were >95% pure as determined by sodium dodecyl sulfate−polyacrylamide gel electrophoresis were passed through a 5 mL Ni-Sepharose HP (GE Healthcare) column to remove uncut protein and TEV protease. Protein not retained by the column was concentrated to 15−30 mg/mL by centrifugal ultrafiltration. Aliquots were snap-frozen in liquid nitrogen and stored at −80 °C.

Cloning, Expression, and Purification of Bamb_1224 from *B. ambifaria* AMMD. The gene for Bamb_1224 was cloned from *B. ambifaria* AMMD (gil115351277) with the primer pair of 5′-GCAGGACCATATGACGTTCCGCATCG-ACGCTCATCAA-3′ and 5′-GCAGGACAAGCTTTTGAGC-GTGTTGATCGCCGGACGGCCGA-3′. Restriction sites for NdeI and HindIII were inserted into the forward and reverse primers, respectively. The PCR product was purified with a

dx.doi.org/10.1021/bi3015554 | *Biochemistry* 2013, 52, 239−253

Scheme 2

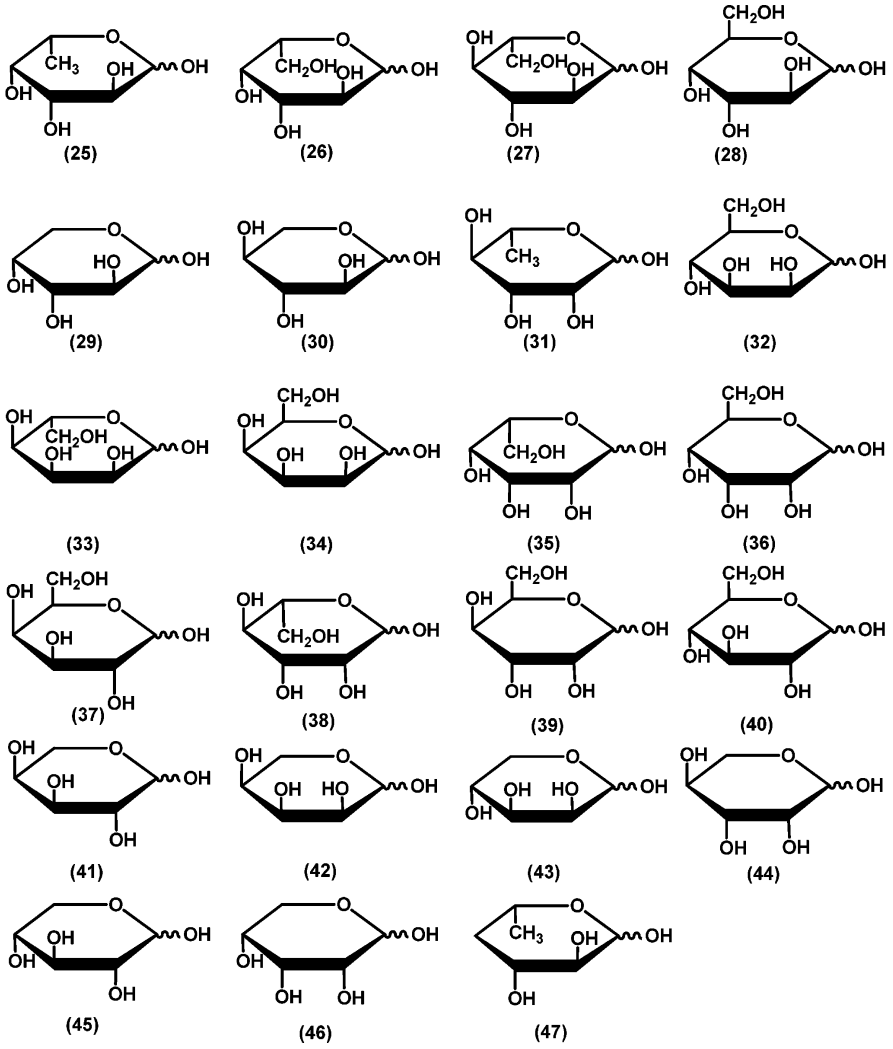

PCR cleanup system (Promega), doubly digested with NdeI and HindIII, and then ligated into a pET-30a(+) vector (Novagen) previously digested with NdeI and HindIII. The recombinant plasmid harboring this gene was transformed into BL21(DE3) cells (Novagen) via electroporation.

A single colony was used to inoculate 5 mL cultures containing LB and 50 μg/mL kanamycin and allowed to grow overnight at 37 °C. The overnight cultures were used to inoculate 1 L of LB medium supplemented with 50 μg/mL kanamycin. These cultures were incubated until the OD_{600} reached 0.4−0.6, and then 1.0 mM isopropyl β-thiogalactoside (IPTG) was added to induce gene expression at ambient temperature (25 °C) for an additional 18 h. Cells were harvested by centrifugation at 4 °C and then resuspended in 20 mM HEPES (pH 7.5). Approximately 0.1 mg/mL phenylmethanesulfonyl fluoride (PMSF) was added to the cell suspension, and then the cells were lysed via multiple rounds of sonication in 50 mM HEPES (pH 7.4), 0.5 M NaCl, and 40 mM imidazole. Nucleic acids were removed from the supernatant solution by the addition of a 2% (w/v) protamine sulfate solution over the course of 30 min at 4 °C. The protamine sulfate-bound DNA was removed by centrifugation at 4 °C, and the supernatant was collected and applied to a 5 mL HisTrap HP (GE Healthcare) nickel affinity column. Protein was eluted from the nickel affinity column with 50 mM HEPES (pH 7.4), 0.5 M NaCl, and 500 mM imidazole over a gradient of 25 column volumes.

Cloning, Expression, and Purification of BmulJ_04919 from *B. multivorans* ATCC 17616. The gene for BmulJ_04919 was cloned from *B. multivorans* ATCC 17616 (gil189353674) with the primer pair of 5′-GCAGGAGCCATATGGATCTGAATCTGCAGGACAAGGTCGT3′ and 5′-GCAGGAGCAAGCTTTCAGACGAGCGCACGATCGAGATGCGTAT-3′. Restriction sites for NdeI and HindIII were inserted into the forward and reverse primers, respectively. The PCR product was purified with a PCR cleanup system (Promega), doubly digested with NdeI and HindIII, and then ligated into a pET-30a(+) vector (Novagen) previously digested with NdeI and HindIII. The recombinant plasmid harboring this gene was transformed into BL21(DE3) cells (Novagen) via electroporation.

A single colony was used to inoculate 5 mL cultures containing LB and 50 μg/mL kanamycin, and the cultures were allowed to grow overnight at 37 °C. The overnight cultures were used to inoculate 1 L of LB medium supplemented with 50 μg/mL kanamycin. These cultures were incubated until the OD_{600} reached 0.4−0.6, and then 1.0 mM IPTG was added to induce gene expression at ambient temperature (25 °C) for an additional 18 h. Cells were harvested by centrifugation at 4 °C and then resuspended in 20 mM HEPES (pH 7.5).

dx.doi.org/10.1021/bi3015554 | *Biochemistry* 2013, 52, 239−253

Approximately 0.1 mg/mL PMSF was added to the cell suspension, and then the cells were lysed via multiple rounds of sonication. Nucleic acids were removed from the supernatant solution by the addition of a 2% (w/v) protamine sulfate solution over the course of 30 min at 0 °C. The protamine sulfate-bound DNA was removed by centrifugation at 4 °C. Solid ammonium sulfate was added to 50% of saturation and the precipitated protein isolated by centrifugation. The protein was resuspended in a minimal amount of 20 mM HEPES (pH 7.5) and then applied to a High Load 26/60 Superdex 200 gel filitration column (GE Healthcare). Fractions containing the protein of expected size were pooled and purified further by ion exchange chromatography with a ResourceQ column (6 mL) at pH 7.5.

Crystallization and Data Collection for BmulJ_04915 and BmulJ_04919. All crystallization experiments were conducted by the sitting drop vapor diffusion method at 18 °C in 96-well Intelliplates (Art Robbins Instruments). Equal volumes of crystallization reagent and protein (0.5 μL each) were mixed and equilibrated against 70 μL of the crystallization agent in the reservoir. Crystals of BmulJ_04915 [30 mg/mL in 20 mM HEPES (pH 7.8), 150 mM NaCl, 5% glycerol, 0.5 mM $ZnCl_2$, and 9 mM TCEP] were obtained with 20% (w/v) PEG 3350 and 100 mM HEPES (pH 7.5). Hexagonal rods (0.2 mm × 0.05 mm × 0.05 mm) grew sporadically over 1−2 months. Crystals were soaked in mother liquor supplemented with 20% (v/v) glycerol for 10 s prior to being flash-cooled in liquid nitrogen. Crystals of unliganded BmulJ_04919 [14.5 mg/mL in 50 mM Tris (pH 7.5)] were obtained with 0.2 M calcium acetate, 10% (w/v) PEG 8000, and 0.1 M HEPES (pH 7.5). Triganol bipyramids appeared in 1−2 days and grew to the maximal size in a week (0.2 mm × 0.1 mm × 0.1 mm). Crystals were soaked in mother liquor supplemented with 20% ethylene glycol for 10 s prior to being flash-cooled in liquid nitrogen. Crystals of the BmulJ_04919 [14.5 mg/mL in 50 mM Tris (pH 7.5), 5 mM $NADP^+$, and 25 mM L-fucose] ternary complex were obtained in 0.2 M $MgCl_2$, 20% (w/v) PEG 8000, and 0.1 M Tris (pH 8.5). Crystals of the ternary complex formed as small (0.05 mm × 0.025 mm × 0.025 mm) misshapen plates that grew at the periphery of the drop over 1−2 weeks. Crystals were soaked in mother liquor supplemented with 5 mM $NADP^+$, 25 mM L-fucose, and 20% (v/v) ethylene glycol for 2 min prior to being flash-cooled in liquid nitrogen. All X-ray diffraction data were collected at 100 K using synchrotron radiation (λ = 0.98), and intensities were integrated with MOSFLM and scaled with SCALA [Protein Data Bank (PDB) entries 4DNM and 4GKB] or HKL3000 (PDB entry 4GVX).[17−19] Data for BmulJ_04915 were collected on a Quantum 315 CCD detector (Area Detector Systems Corp.) at NSLS beamline X29A (National Synchrotron Light Source, Brookhaven National Laboratory, Upton, NY). Data for BmulJ_04919 were collected on a Rayonix 225-HE detector (Rayonix) at APS beamline 31-ID (Advanced Photon Source, Argonne National Laboratory, Argonne, IL).

Determination of the Structure of BmulJ_04915 and BmulJ_04919. Initial phases for BmulJ_04915 were determined by molecular replacement (MR) using PHENIX/PHASER and a monomeric ensemble model generated by an overlay of the structures represented by PDB entries 2QAH, 2FFI, and 3CJP, all homologues with sequences that are <20% identical.[20,21] Starting with the MR phases, we were able with the autobuild wizard of PHENIX to build a majority of the structure with R and R_{free} values of 26.9 and 30.8%, respectively. Initial phases for unliganded BmulJ_04919 were determined by MR using MOLREP and a tetrameric search model (PDB entry 3FTP).[22] A BmulJ_04919 homology model, constructed utilizing the SWISSPDB homology modeling server, was subsequently placed according to the MOLREP MR solution.[23] This model was subjected to simulated annealing using torsion angle dynamics within PHENIX, generating an initial model with R and R_{free} values of 39.2 and 42.5%, respectively. The structure of the NADP−L-fucose−BmulJ_04919 ternary complex was determined using a single subunit of the unliganded complex. Iterative cycles of refinement in PHENIX and model building in COOT were utilized to obtain the final crystallographic structures.[24] Ligand geometry restraints were built using ELBOW within PHENIX.

Measurement of Enzyme Activity. The enzymatic hydrolysis of lactones was monitored with a SpectraMax340 UV−visible spectrophotometer using a colorimetric pH indicator assay at 30 °C. Protons released from the carboxylate product during lactone hydrolysis were measured using the pH indicator cresol purple or bromothymol blue.[25] Reaction mixtures measured with cresol purple contained 2.5 mM BICINE buffer (pH 8.3), 0.2 M NaCl, 0−1.0 mM lactone, 0.1 mM cresol purple, and the lactonase. Reaction mixtures measured with bromothymol blue contained 2.5 mM MOPS buffer (pH 7.1), 0.2 M NaCl, 0−0.5 mM lactone, and 0.1 mM bromothymol blue. The final concentration of DMSO was 1%. Changes in absorbance at 577 nm (ε = 1764 M^{-1} cm^{-1}) and 616 nm (ε = 1135 M^{-1} cm^{-1}) were monitored in 96-well plates for cresol purple and bromothymol blue, respectively. Background rates arising from acidification by atmospheric CO_2 were observed and subtracted from the initial rates. The dehydrogenase activity catalyzed was monitored with a SpectraMax340 UV−visible spectrophotometer by measuring the reduction of $NADP^+$ or NAD^+ at 340 nm (ε = 6220 M^{-1} cm^{-1}) at 30 °C. The assays were performed in 50 mM BICINE buffer (pH 8.0), varying concentrations of sugar substrates, and 0.5 mM $NADP^+$. Kinetic constants for $NADP^+$ and NAD^+ were determined in the same manner as described above except that the assay conditions were as follows: 50 mM BICINE buffer (pH 8.0), varying concentrations of nucleotide, and 200 μM L-fucose.

Data Analysis. The kinetic constants were determined from a fit of the initial velocity data to eq 1 using the nonlinear least-squares fitting program in SigmaPlot 9.0

$$\nu/E_t = (k_{cat}[A])/(K_m + [A]) \quad (1)$$

where ν is the initial velocity, E_t is the total enzyme concentration, k_{cat} is the turnover number, [A] is the substrate concentration, and K_m is the Michaelis constant.

Metal Analysis. The metal content of BmulJ_04915 was determined with an Elan DRC II ICP-MS instrument as previously described.[26] Protein samples for ICP-MS analysis were digested with HNO_3 and then refluxed for 30 min.[27] All buffers were passed through a column of Chelex 100 (Bio-Rad) to remove trace metal contamination. EDTA and 1,10-phenanthroline (1.0 mM) were incubated with 1.0 μM BmulJ_04915 in 50 mM buffer at pH values ranging from 6 to 10 to remove divalent metal ions. The buffers for these experiments included CHES (pH 6.0), HEPES (pH 7.0), BICINE (pH 8.0), and CHES (pH 9.0 and 10.0). The effect of added divalent cations on the catalytic activity of BmulJ_04915 was determined by adding Mn^{2+}, Zn^{2+}, Co^{2+}, Cu^{2+}, or Ni^{2+} (0−500 μM) directly to the assay mixtures. The purified enzyme

Table 1. Catalytic Constants for BmulJ_04915, Bamb_1224, and Patl_0798

	BmulJ_04915			Bamb_1224			Patl_0798		
compound	k_{cat} (s^{-1})	K_m (mM)	k_{cat}/K_m (M^{-1} s^{-1})	k_{cat} (s^{-1})	K_m (mM)	k_{cat}/K_m (M^{-1} s^{-1})	k_{cat} (s^{-1})	K_m (mM)	k_{cat}/K_m (M^{-1} s^{-1})
				At pH 8.3					
L-fucono-1,4-lactone (**1**)	140 ± 8	1.4 ± 0.2	1.0 (0.1) × 10^5	89 ± 4	0.9 ± 0.1	1.0 (0.1) × 10^5	139 ± 6	1.2 ± 0.1	1.2 (0.2) × 10^5
L-galactono-1,4-lactone (**2**)	32 ± 2	1.1 ± 0.2	3.0 (0.3) × 10^4	55 ± 2	1.3 ± 0.1	4.0 (0.3) × 10^4	119 ± 7	1.5 ± 0.2	8.0 (0.5) × 10^4
D-arabinono-1,4-lactone (**6**)	59 ± 2	0.7 ± 0.05	8.4 (0.5) × 10^4	19 ± 1	0.8 ± 0.1	2.4 (0.2) × 10^4	25 ± 3	0.75 ± 0.02	3.3 (0.2) × 10^4
L-xylono-1,4-lactone (**7**)	14 ± 1	1.5 ± 0.3	1.0 (0.1) × 10^4	6.0 ± 0.5	1.3 ± 0.3	5.0 (0.5) × 10^3	10 ± 0.3	1.5 ± 0.4	6.6 (0.2) × 10^4
4-deoxy-L-fucono-1,5-lactone (**24**)	ND[a]	ND[a]	ND[a]	ND[a]	ND[a]	ND[a]	ND[a]	ND[a]	ND[a]
				At pH 7.1					
L-fucono-1,4-lactone (**1**)	4.0 ± 0.1	0.6 ± 0.1	7 (0.1) × 10^4	4.1 ± 0.3	0.9 ± 0.1	5.0 (0.1) × 10^3	3.0 ± 0.2	0.6 ± 0.1	4.5 (0.5) × 10^3
L-galactono-1,4-lactone (**2**)	6.0 ± 0.5	1.3 ± 0.2	5.0 (0.5) × 10^3	6.2 ± 2.0	0.5 ± 0.1	4.0 (0.5) × 10^3	5.7 ± 0.3	2.6 ± 0.3	2.2 (0.1) × 10^3
D-arabinono-1,4-lactone (**6**)	2.0 ± 0.2	1.0 ± 0.3	1.6 (0.3) × 10^3	2.2 ± 0.2	0.7 ± 0.1	3.2 (0.2) × 10^3	1.8 ± 0.2	1.6 ± 0.3	1.0 (0.1) × 10^3
L-xylono-1,4-lactone (**7**)	ND[a]	ND[a]	1.0 (0.1) × 10^3	ND[a]	ND[a]	7.0 (0.3) × 10^2	ND[a]	ND[a]	1.0 (0.2) × 10^3
4-deoxy-L-fucono-1,5-lactone (**24**)	994 ± 64	0.13 ± 0.03	8.0 (1.0) × 10^6	1530 ± 47	0.21 ± 0.02	7.2 (0.6) × 10^6	1320 ± 80	0.45 ± 0.02	2.6 (0.2) × 10^6

[a]Kinetic constants were not determined for this substrate.

was also incubated with 50−500 molar equiv of these divalent cations for 24 h at 4 °C in 50 mM HEPES (pH 7.5) and subsequently assayed for catalytic activity.

Reaction Product of BmulJ_04919 with L-Fucose. The product of the reaction catalyzed by BmulJ_04919 was determined through ^1H, ^{13}C heteronuclear multiple-bond correlation (HMBC) and correlation nuclear magnetic resonance (NMR) spectroscopy using a Bruker Avance III 500 MHz spectrometer with an H, C, N cryoprobe. WATERGATE solvent suppression was performed on reaction samples in 500−1000 μL of D_2O with 100 mM acetate buffer (pH 5.5), 25 mM NAD^+, 25 mM L-fucose, and 100 μM BmulJ_04919. After being incubated for 10 min, the enzyme was removed from the reaction mixture using a 3 kDa cutoff VWR centrifugal filter. NAD^+ and NADH were removed by the addition of Dowex-1 X2 anion exchange resin that was previously equilibrated with 50 mM acetate buffer (pH 5.5). The pH of the sample was then adjusted to pH 4.2 with 1 M acetate buffer (pH 4.2).

L-Fucono-1,5-lactone was identified as a substrate for BmulJ_04915 using ^1H NMR spectroscopy. The reactions were conducted with 50 mM phosphate buffer (pH 6.5), 15 mM L-fucose, 15 mM NAD^+, 10 μM BmulJ_04919, and 10 μM BmulJ_04915 in a final reaction volume of 200 μL. ^1H NMR spectra were recorded over 1 min intervals with WATERGATE solvent suppression.

Enzymatic Synthesis of 4-Deoxy-L-fucono-1,5-lactone. 4-Deoxy-L-fucono-1,5-lactone (**24**) was synthesized enzymatically from 4-deoxy-L-fucose (**47**) using BmulJ_04919 as the catalyst. The reaction was conducted in 50 mM phosphate buffer (pH 7.0), 15 mM 4-deoxy-L-fucose, and 15 mM NAD^+ in a final volume of 1 mL for 20 min. The enzyme was removed from the reaction mixture using a 3 kDa cutoff VWR centrifugal filter. NAD^+ and NADH were removed by the addition of Dowex-1 X2 anion exchange resin. The structure of the lactone was determined using HMBC and correlation NMR spectroscopy with a Bruker Avance III 500 MHz spectrometer with an H, C, N cryoprobe using WATERGATE solvent suppression

Sequence Similarity Network for cog3618. Proteins belonging to cog3618 were identified from the NCBI protein database using the query "cog3618". The proteins within cog3618 were subjected to an all-by-all BLAST at a specified *E* value (10^{-50}, 10^{-60}, etc.) using the NCBI standalone BLAST program. The BLAST files were opened and visualized in the similarity network program Cytoscape.[28]

RESULTS

Purification of BmulJ_04915. The gene for BmulJ_04915 was cloned and expressed in *Escherichia coli*, and the protein was purified to homogeneity. The purified enzyme contained ~0.7 molar equiv of Zn^{2+}. The addition of chelating agents or divalent metal ions (Mn^{2+}, Zn^{2+}, Co^{2+}, Cu^{2+}, or Ni^{2}) directly to the assay mixture did not affect the rate of enzyme-catalyzed hydrolysis of L-fucono-1,4-lactone (**1**). The purified enzyme was incubated with EDTA or 1,10-phenanthroline at pH values ranging from 6 to 10 to chelate the metal ions bound to the protein. The addition of chelators did not diminish the catalytic activity of this enzyme, and ICP-MS analysis demonstrated that the addition of 1,10-phenanthroline removed >95% of the Zn^{2+} that was initially bound to the protein. The apoenzyme had the same catalytic activity as the as-purified enzyme. Therefore, BmulJ_04915 does not require a divalent cation for substrate turnover.

Substrate Specificity. BmulJ_04915 is a member of cog3618 from the amidohydrolase superfamily. Other enzymes from cog3618 have been shown to catalyze the hydrolysis of lactones.[7−9] The genomic context is indicative of an enzyme that participates in the metabolism of carbohydrates, and thus, this enzyme was predicted to catalyze the hydrolysis of sugar lactones. The enzyme was screened against a small and focused library of 23 lactones as potential substrates for this enzyme (see Scheme 1). BmulJ_04915 exhibited catalytic activity for the hydrolysis of L-fucono-1,4-lactone (**1**), D-arabino-1,4-

dx.doi.org/10.1021/bi3015554 | *Biochemistry* 2013, 52, 239−253

Table 2. Data Collection and Refinement Statistics for the BmulJ_04915 and BmulJ_04919 Crystal Structures

	BmulJ_04915	apo-BmulJ_04919	BmulJ_04919 Ternary complex
		Data Collection[a]	
space group	$P3_221$	$P6_1$	$C2$
unit cell	a = 75.1 Å, c = 142.3 Å	a = 100.0 Å, c = 205.8 Å	a = 68.4 Å, b = 118.5 Å, c = 118.2 Å, β = 92.9°
resolution (Å)	40−2.15 (2.27−2.15)	40−1.5 (1.52−1.50)	40−1.5 (1.52−1.5)
completeness (%)	99.9 (99.8)	100.0 (100.0)	96.7 (98.7)
redundancy	11.4 (11.7)	8.9 (9.3)	2.8 (2.7)
mean(I)/sd(I)	17.3 (3.5)	10.8 (2.8)	10.0 (1.8)
R_{sym}	0.094 (0.777)	0.110 (0.836)	0.103 (0.494)
		Structure	
resolution (Å)	40−2.15 (2.23−2.15)	40−1.5 (1.52−1.50)	40−1.5 (1.52−1.50)
no. of unique reflections	25899 (2790)	185136 (6256)	145306 (4808)
R_{cryst} (%)	19.0 (25.3)	15.1 (23.4)	15.2 (20.3)
R_{free} (%, 5% of data)	22.8 (28.9)	17.2 (24.9)	17.9 (22.7)
contents of model (native range)[b]	1−296	1−258	1−258
observed residues	3−289	A1−191, A203−258, B1−258, C1−258, D1−194, D203−258	A1−258, B1−258, C1−258, D1−258
waters	194	1098	1045
all atoms	2526	8876	9232
average B factor (Å^2)			
Wilson B Factor (Å^2)	25.6	13.8	8.9
TLS groups	11.0	14.0	25.0
protein/water/NADP/fucose	30.6/39.8/−/−	14.1/29.1/−/−	9.4/23.9/7.7/6.8
rmsd for bond lengths (Å)	0.01	0.008	0.006
rmsd for bond angles (deg)	1.11	1.12	1.17
MOLPROBITY statistics			
Ramachandran favored/outliers (%)	98.6 (0.35)	96.9 (0.0)	96.9 (0.0)
Ramachandran rotamer outliers (%)	1.4	1.4	1.4
Clashscore[c]	8.38 (91st percentile)	5.37 (91st percentile)	3.81 (95th percentile)
overall score[c]	1.56 (97th percentile)	1.59 (78th percentile)	1.47 (87th percentile)
PDB entry	4DNM	4GKB	4GVX

[a]Statistics in parentheses are for the highest-resolution bin. [b]Numbers outside of the listed native range are polyhistidine tags or cloning artifacts. [c]Scores are ranked according to structures of similar resolution as formulated in MOLPROBITY.

lactone (**6**), L-xylono-1,4-lactone (**7**), and L-galactono-1,4-lactone (**2**). The best substrate from this initial set of compounds is L-fucono-1,4-lactone. The kinetic constants are listed in Table 1.

Structure of BmulJ_04915. The structure of BmulJ_04915 was determined by molecular replacement to 2.15 Å resolution (Table 2). There is a monomer in the asymmetric unit that is consistent with the protein being a monomer in solution. The final model contains residues 3−289, all of which are well-defined in electron density. The crystal from which BmulJ_04915 was determined requires TCEP and Zn^{2+} (added prior to the knowledge that BmulJ_04915 was not a metalloenzyme) to form and was only sporadically reproducible. A well-defined Zn^{2+} ion, coordinated by Asp-176 and His-222 of one molecule and Cys-71 and Asp-72 of a crystallographically related molecule, specifies how Zn^{2+} was critical to the crystallization. BmulJ_04915 forms a distorted $(\beta/\alpha)_8$ TIM barrel with an active site at the C-terminal end of the β-barrel consistent with other members of the amidohydrolase family (Figure 4A). There are few inserted secondary structural elements, with most of the defining structural features being extended loops connecting the $(\beta/\alpha)_8$ TIM barrel elements. Residual density within the active site was modeled as a bound HEPES molecule derived from crystallization buffer. The piperazine ring lies against the face of Trp-22 (loop between β-strand 1 and α-helix 1), while the sulfonate is interacting with Arg-106 and the three active site histidine residues (His-9, His-11, and His-166) (Figure 4B). A search using the SSM server returns a number of amidohydrolases at >2.0 Å root-mean-square deviation (rmsd) and <20% sequence identity, demonstrating that the structure of BmulJ_04915 is significantly different from those previously determined.[29] The closest structure is that of the 2-pyrone-4,6-dicarboxylic acid hydrolase (LigI) from *Sphingomonas paucimobilis* (rmsd of 2.2 Å over 229 Cα atoms, 20% sequence identity), which also catalyzes the hydrolysis of a lactone.[7]

Purification and Properties of BmulJ_04919. A gene for a protein currently annotated as a short chain dehydrogenase of

dx.doi.org/10.1021/bi3015554 | *Biochemistry* 2013, 52, 239−253

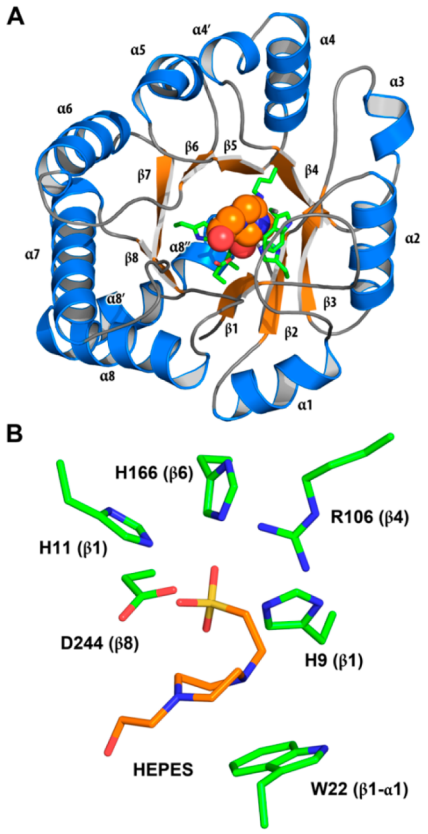

Figure 4. Structure of BmulJ_04915. (A) Ribbon diagram of BmulJ_04915. The HEPES molecule is shown as spheres. (B) Residues directly adjacent to bound HEPES in the active site of BmulJ_04915. Numbers in parentheses designate the approximate location in the secondary structure from which the residue originates.

unknown specificity (BmulJ_04919) is positioned in the same putative operon as BmulJ_04915. This gene was cloned and overexpressed and the protein purified to homogeneity. BmulJ_04919 is a member of cog1028, which includes other enzymes with the following experimentally verified functions: 2-dehydro-3-deoxy-L-fuconate dehydrogenase,[11] 2-dehydro-3-deoxy-L-rhamnonate dehydrogenase,[9] L-rhamnose dehydrogenase,[9] 2,3-dihydro-2,3-dihydroxybenzoate dehydrogenase,[30] D-gluconate dehydrogenase,[31] and sorbitol-6-phosphate dehydrogenase.[32] The closest homologue to BmulJ_04919 with a verified catalytic activity in cog1028 appears to be L-rhamnose dehydrogenase from *Sphingomonas* sp. SKA58. BmulJ_04919 is unrelated to the putative L-fucose dehydrogenase (XCC4065 from *X. campestris*) from cog0667.[11,33] The oxidized product of the reaction catalyzed by BmulJ_04919 is likely to be the physiological substrate for BmulJ_04915.

Substrate Specificity of BmulJ_04919. It was anticipated that BmulJ_04919 would catalyze the formation of L-fucose-1,5-lactone from L-fucose and $NADP^+$ because the pyranose form of L-fucose is predominant in solution (Figure 6A). To determine the substrate specificity of this enzyme, a small library of pentose and hexose sugars was tested as potential substrates by monitoring the reduction of $NADP^+$ at 340 nm (Scheme 2). L-Fucose (**25**), L-galactose (**26**), and D-arabinose (**29**) were the only sugars oxidized by this enzyme. The dehydrogenase has the highest activity with L-fucose, and the kinetic constants are listed in Table 3.

Table 3. Catalytic Constants for BmulJ_04919 at pH 8.0[a]

substrate	k_{cat} (s^{-1})	K_m (μM)	k_{cat}/K_m (M^{-1} s^{-1})
L-fucose (**25**)	10 ± 0.3	6.2 ± 0.8	1.5 (0.2) × 10^6
D-arabinose (**29**)	21.0 ± 0.1	94 ± 3	2.3 (0.1) × 10^5
L-galactose (**26**)	11 ± 0.5	285 ± 36	3.7 (0.3) × 10^4
4-deoxy-L-fucose (**47**)	26 ± 1	786 ± 92	4.0 (0.1) × 10^4
$NADP^+$	11 ± 0.2	4.0 ± 0.5	3.0 (0.4) × 10^6
NAD^+	15 ± 1	28 ± 4	5.3 (0.1) × 10^5

[a]When $NADP^+$ or NAD^+ was varied, the L-fucose concentration was fixed at 200 μM. When the sugar substrates were varied, the $NADP^+$ concentration was fixed at 500 μM.

Identification of the Initial Reaction Product of BmulJ_04919. The only product of an L-fucose dehydrogenase that has ever been structurally characterized is L-fucono-1,4-lactone (**1**).[35] However, it has been proposed that L-fucono-1,5-lactone is the true product of the reaction, but this compound has never been observed because of the rapid nonenzymatic conversion to L-fucono-1,4-lactone (**1**) or hydrolysis to L-fuconate.[34,35] To help stabilize product formation, the reaction was conducted at pH 5.5 and then quenched at pH 4.2. The initial product was structurally characterized by NMR spectroscopy and shown to be L-fucono-1,5-lactone with the resonance for the methyl group at 1.32 ppm, which quickly rearranges to the 1,4-lactone (1.24 ppm) at pH >5.0. For further characterization, the reaction was quenched at pH 4.2, which greatly slowed the intermolecular rearrangement.

The enzymatically produced L-fucono-1,5-lactone is rapidly converted to L-fucono-1,4-lactone (**1**). Enzyme, NAD^+, and L-fucose were added together at pH 5.5, and the reaction was monitored by ^{1}H NMR spectroscopy until L-fucono-1,5-lactone was the predominate product. The enzyme was removed from the reaction mixture and the pH adjusted to 6.5. The time course for the subsequent change in the ^{1}H NMR spectrum for the C-6 methyl groups of L-fucose (**25**) and the reaction products is presented in Figure 5. At 1.1 and 1.2 ppm, there is a pair of doublets for the α- and β-anomers of L-fucose (**25**). At 1.24 and 1.32 ppm are the two doublets for L-fucono-1,4-lactone (**1**) and L-fucono-1,5-lactone, respectively (Figure 5A). At the earliest time points, L-fucono-1,5-lactone is clearly dominant versus L-fucono-1,4-lactone (**1**). However, after 5 min, approximately half of the L-fucono-1,5-lactone has been converted to the L-fucono-1,4-lactone (Figure 5B). After 1 h, nearly all of the L-fucono-1,5-lactone was converted to L-fucono-1,4-lactone (**1**) (Figure 5C). The nonenzymatic transformation of L-fucono-1,5-lactone to L-fucono-1,4-lactone (**1**) does not utilize the hydrolyzed product, L-fuconate, as a reactive intermediate. The rate constant is approximately 0.12 min^{-1} at pH 6.5.

Identification of the Physiological Substrate for BmulJ_04915. To determine whether BmulJ_04915 preferentially hydrolyzes the 1,4- or 1,5-lactone of L-fuconate, BmulJ_04919 was incubated with L-fucose (**25**) and NAD^+. Shown in Figure 6A is the ^{1}H NMR spectrum of the methyl carbon for the α- and β-anomers of L-fucose (**25**) before the addition of BmulJ_04919. After ~5 min, the concentrations of the two lactones were approximately equal as shown in Figure 6B. The lactonase (BmulJ_04915) was added, and the spectrum of the reaction product was monitored as a function of time. The resonances for the L-fucono-1,5-lactone disappeared at a significantly higher rate than those for L-fucono-

dx.doi.org/10.1021/bi3015554 | *Biochemistry* 2013, 52, 239−253

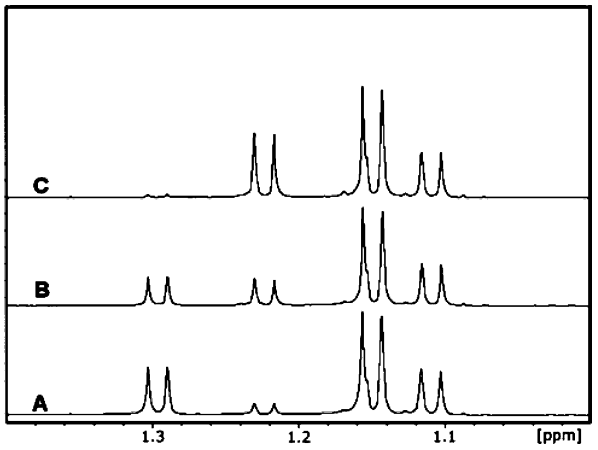

Figure 5. ^{1}H NMR time course for the nonenzymatic conversion of L-fucono-1,5-lactone to L-fucono-1,4-lactone. The resonances corresponding to the C-6 methyl groups of both α-L-fucose (1.12 ppm) and β-L-fucose (1.15 ppm), L-fucono-1,5-lactone (1.32 ppm), and L-fucono-1,4-lactone (1.24 ppm) are presented. (A) The major reaction product of BmulJ_04915 at pH 4.2 is shown to be L-fucono-1,5-lactone. (B) Five minutes after the reaction mixture had been adjusted to pH 6.5, the L-fucono-1,4-lactone is at a concentration equal to that of the original enzymatic product. (C) Sixty minutes after the pH of the reaction mixture had been adjusted to pH 6.5, the major peak is L-fucono-1,4-lactone.

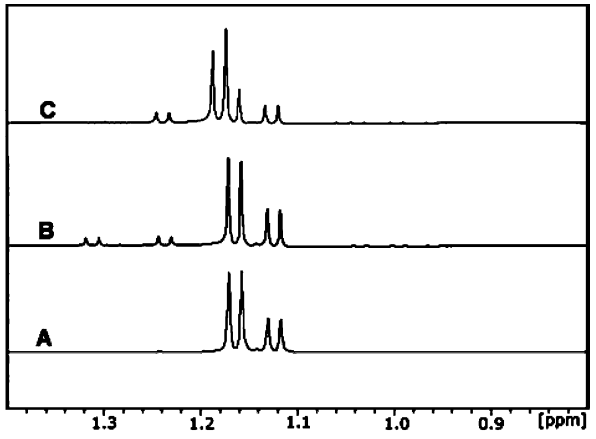

Figure 6. ^{1}H NMR time course of the enzymatic conversion of L-fucose to L-fucono-1,5-lactone and L-fucono-1,5-lactone to L-fuconate. The resonances corresponding to the C-6 methyl groups of both α-L-fucose (1.125 ppm) and β-L-fucose (1.15 ppm), L-fucono-1,5-lactone (1.295 ppm), L-fucono-1,4-lactone (1.225 ppm), and L-fuconate (1.182 ppm) are provided. (A) L-Fucose, the substrate for BmulJ_04919, prior to addition of the enzyme at pH 6.5. (B) Five minutes after the addition of BmulJ_04919 to L-fucose, the enzymatic product, L-fucono-1,5-lactone, and the nonenzymatic product, L-fucono-1,4-lactone, are at equal concentrations. (C) Five minutes after the addition of BmulJ_04915 to the reaction mixture, the L-fucono-1,5-lactone is no longer present in the reaction mixture and the L-fucono-1,4-lactone appears to be unchanged. L-Fuconate (1.182 ppm) appears to be the major product. The α-anomer of L-fucose appears to be unchanged; however, the concentration of the β-anomer has been reduced to at least half of the original value.

1,4-lactone (**1**) (Figure 6C). The formation of L-fuconate was confirmed by the new resonance at approximately 1.18 ppm.

To further demonstrate that BmulJ_04915 catalyzes the hydrolysis of the 1,5-lactone faster than the 1,4-lactone, 4-deoxy-L-fucono-1,5-lactone (**24**) was synthesized enzymatically using 4-deoxy-L-fucose (**47**) as a substrate for BmulJ_04919. This compound is missing the hydroxyl group at C-4 and thus cannot form a 1,4-lactone. The product of this reaction was shown to be 4-deoxy-L-fucono-1,5-lactone (**24**) by NMR spectroscopy (Figure 7A). As no 4-hydroxyl group is available,

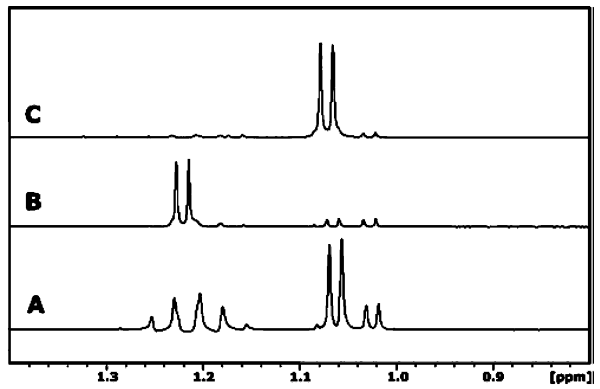

Figure 7. ^{1}H NMR time course of the enzymatic conversion of 4-deoxy-L-fucose to 4-deoxy-L-fucono-1,5-lactone and 4-deoxy-L-fuconate. The resonances corresponding to the C-6 methyl groups of both α-4-deoxy-L-fucose (1.02 ppm) and β-4-deoxy-L-fucose (1.06 ppm), 4-deoxy-L-fucono-1,5-lactone (1.25 ppm), and 4-deoxy-L-fuconate (1.07 ppm) are provided. (A) 4-Deoxy-L-fucose, prior to addition of enzymes at pH 6.5. (B) One minute after the addition of BmulJ_04919 to 4-deoxy-L-fucose, the enzymatic product is 4-deoxy-L-fucono-1,5-lactone. (C) One minute after the addition of BmulJ_04915 to the reaction mixture, 4-deoxy-L-fucono-1,5-lactone is no longer present in the reaction mixture and 4-deoxy-L-fuconate (1.07 ppm) appears to be the major product.

the six-member lactone is relatively stable and undergoes slow nonenzymatic hydrolysis. A new methyl doublet appears at 1.25 ppm when 4-deoxy-L-fucose is oxidized to 4-deoxy-L-fucono-1,5-lactone by BmulJ_04919 (Figure 7B). After hydrolysis with BmulJ_04915, this resonance disappears and the methyl resonance for 4-deoxy-L-fuconate appears at 1.07 ppm (Figure 7C). The 4-deoxy-L-fucono-1,5-lactone (**24**) was isolated, and the kinetic constants for the hydrolysis of this compound by BmulJ_04915, Bamb_1224, and Patl_0798 were determined at pH 7.1. The values of k_{cat} and k_{cat}/K_m for the hydrolysis of 4-deoxy-L-fucono-1,5-lactone are approximately 250- and 115-fold greater, respectively, than those for L-fucono-1,4-latone assayed at pH 7.1 (Table 1).

Structure of BmulJ_04919. Unliganded BmulJ_04919 crystallized in space group $P6_1$ with a tetramer per asymmetric unit and was phased by molecular replacement using a tetrameric model [PDB entry 3FTP, 3-ketoacyl(acyl carrier protein) reductase] and refined to a resolution of 1.5 Å (Table 2). The NADP−L-fucose−BmulJ_04919 ternary complex crystallized in space group C2 with two dimers per asymmetric unit and was phased by molecular replacement using a single subunit of the unliganded structure and refined to a resolution of 1.5 Å. The density was sufficient to build the entire structure, excluding a portion of a helix−turn−helix motif (residues ~192−202) in two subunits of the unliganded structure. The subunit structure of BmulJ_04919 consists mainly of a Rossmann fold dinucleotide cofactor binding motif in which a central, twisted β-sheet consisting of seven parallel β-strands (3-2-1-4-5-6-7 strand topology) is flanked by five helices (α1−α3, α7, and α9) on one side and four helices (α3−α6) on the other (Figures 8). A structure similarity search utilizing the

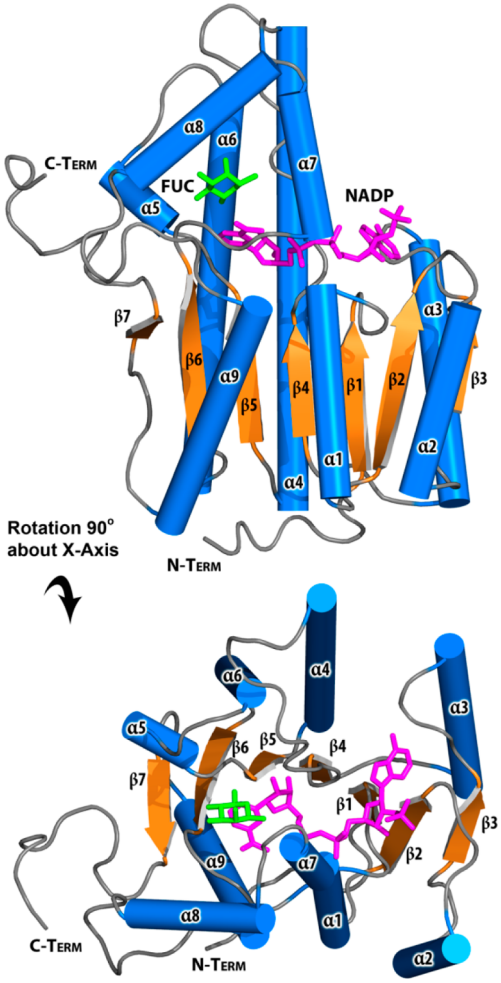

Figure 8. Ribbon diagram of BmulJ_04919 with bound NADP (magenta sticks) and L-fucose (green sticks).

SSM server indicates a similarity to a number of short chain dehydrogenase/reductase (SDR) family enzymes with an rmsd of <1.5.[29] The highest scores were for human retinal short chain dehydrogenase/reductase (PDB entry 1YDE, rmsd of 1.15 Å, sequence identity of 35%, *Z* score of 16.2) and *Thermoplasma acidophilum* D-aldohexose dehydrogenase, AldT (PDB entry 2DTE, rmsd of 1.31 Å, sequence identity of 32%, *Z* score of 15.3). Structurally, the largest differences between these enzymes are modest deviations in the positions of the $\beta4-\alpha4$ loop, $\alpha4$, the $\alpha7/\alpha8$ helix−turn−helix motif, and $\alpha2$. For example, in AldT, $\alpha2$ is converted to a loop and 10 residues are deleted compared to the same region in BmulJ_04919.[36] Examination of the intermolecular interactions of BmulJ_04919 within the two crystal forms is consistent with BmulJ_04919 existing as a tetramer in solution (Figure S1 of the Supporting Information). In addition, the top structural homologues as indicated by the SSM search also exist as similar tetramers in their crystal structures. The tetramer is composed of a dimer of dimers with 222 point group symmetry where the majority of interactions are between the A and B subunits and the A and D subunits. There are only minor interactions between the A and C subunits, where the C-terminus of the A subunit interacts with the C-terminus of the C subunit and $\alpha5$ forming one wall of the L-fucose binding pocket (Figure S1 of the Supporting Information). Interestingly, the C-terminus of AldT was found to cover the sugar binding pocket entirely and was postulated to stabilize the active site conformation and promote the catalytic reaction, with possibly enhanced dissociation at thermophilic temperatures.[36] In contrast, the C-terminus of BmulJ_04919 remains 6−7 Å from the sugar binding pocket and appears to be well-anchored, suggesting it does not move during the reaction.

$NADP^+$ Binding Site of BmulJ_04919. Clear and continuous electron density for $NADP^+$ was visualized in the BmulJ_04919 ternary complex (Figure 9A). As is common in SDR enzymes, the $NAD(P)^+$ is bound at the C-terminal edge of the seven-stranded β-sheet in an extended conformation (Figure 9B).[37] In addition to the general topology, the Rossman fold also includes a highly variable Gly-rich sequence essential for coordination of the cofactor pyrophosphate. In BmulJ_04919, this sequence lies between the end of β-strand 1 and the start of α-helix 1 with the sequence G_{14}GASGIGG$_{21}$. Clear binding determinants that support the preference of BmulJ_04919 for $NADP^+$ over NAD^+ can be identified. The 2′-phosphate of $NADP^+$ forms a salt bridge with the guanidinium group of Arg-39 and a hydrogen bond with the side chain of His-40, both originating from the loop between $\beta2$ and $\alpha2$ (Figure 9C). Utilization of this loop for cofactor discrimination is typical for SDR enzymes.[37] Arg-39 is positioned by a hydrogen bond to Glu-63, originating from the loop between β-strand 3 and α-helix 3. The side chain of Arg-39 additionally stacks against the face of the adenosine moiety, which in combination with van der Walls contacts with Leu-64 and a hydrogen bond from Glu-63 to the adenosine amino group completes the binding pocket for the adenosine moiety.

L-Fucose Binding Site of BmulJ_04919. Clear and continuous electron density was observed for L-fucose (Figure 9D). The unliganded structure superimposes well with the ternary complex with an rmsd of 0.22 Å for 247 common Cα atoms excluding residues 192−202, which are either missing or more distant from the active site in the unliganded structure (see below). The binding site for L-fucose utilizes structural elements from the C-terminal region. L-Fucose binds in a C3-endo conformation and is highly coordinated, with each hydroxyl forming at least two hydrogen bonds to protein atoms (Figure 9E). L-Fucose is bound with C-3 positioned directly against the nicotinamide (3.3 Å) for the 4-*pro-S* hydride transfer typical of "classical" SDR enzymes.[37] In addition, the protein relay connecting the acid/base hydroxyl-tyrosinate (Tyr-163) to a lysine (Lys-157) to a conserved water molecule stabilized by Asn-113, again typical of classical SDR enzymes, is observed.[37] Determinants that are unique to L-fucose binding include Asn-94 from the $\beta4-\alpha4$ loop coordinating the hydroxyl at C-4, Gln-147 from the $\alpha5-\alpha6$ loop coordinating the hydroxyl groups at positions C-3 and C-4, the backbone carbonyl of Ala-184 and the side chain of Glu-185 ($\beta6-\alpha7$ loop) coordinating the hydroxyl groups at positions C-2 and C-3, respectively, and Lys-141 from the N-terminal end of $\alpha5$ coordinating both hydroxyl groups at C-2 and C-3. In addition, the side chains of Asn-94, Leu-190, Tyr-191, and Trp-194 form a hydrophobic pocket that interacts with the methylene group of L-fucose. Indeed, the largest structural change from the apo structure to the ternary complex is the movement of the $\alpha7-\alpha8$ loop to optimize these interactions. In the apo structure, this region either is disordered or is some 3−4 Å more distant from the L-fucose binding site. As $\alpha7$ also interacts with the $NADP^+$ and most SDR reaction mechanisms proceed through an ordered "bi-bi" mechanism [$NAD(P)^+$ binding first and leaving last], one can envision $NADP^+$ binding initiating the

dx.doi.org/10.1021/bi3015554 | *Biochemistry* 2013, 52, 239−253

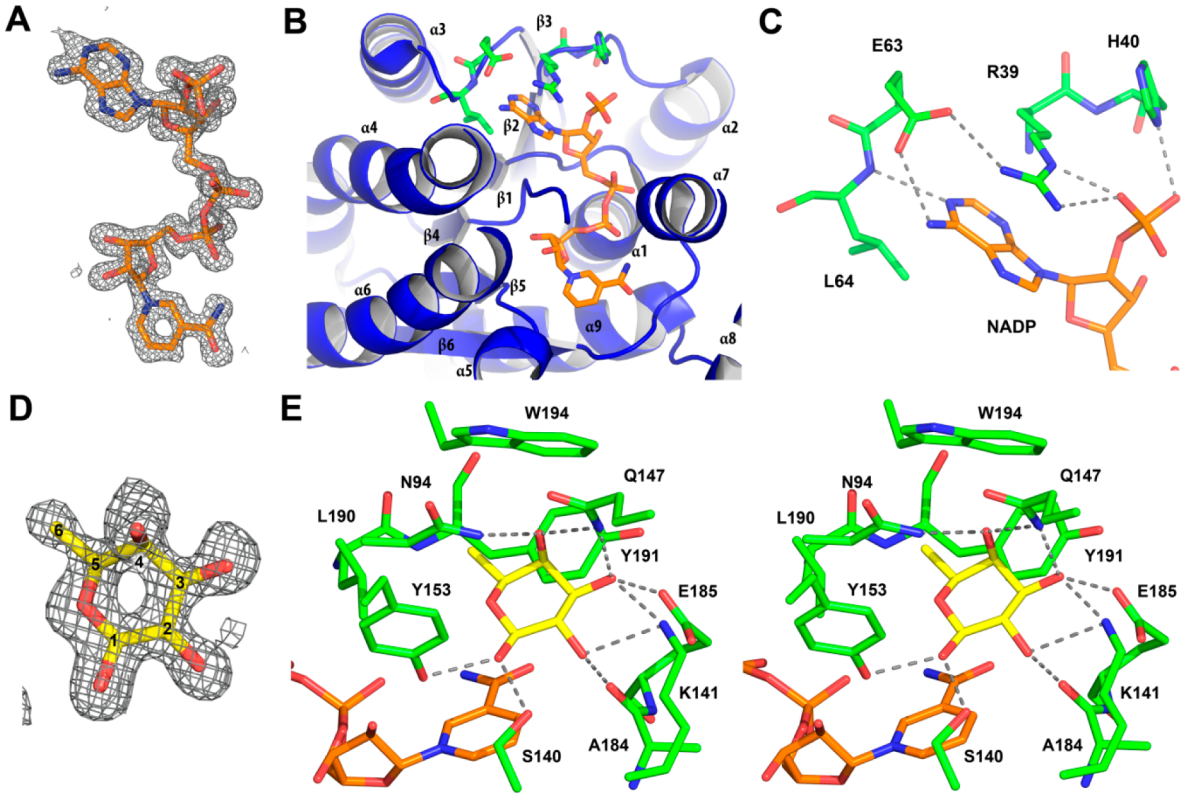

Figure 9. Interactions of BmulJ_04919 with ligands. (A) The 2.5σ $F_o - F_c$ kick map for $NADP^+$ bound to the $NADP^+$–L-fucose–BmulJ_04919 ternary complex. (B) Interactions of $NADP^+$ with the secondary structure elements of BmulJ_04919. (C) 2′-Adenosine phosphate binding site of BmulJ_04919. $NADP^+$ is shown as sticks with orange carbons, and residues of BmulJ_04919 adjacent to the 2′-adenosine phosphate are shown as sticks with green carbons. (D) The 2.5σ $F_o - F_c$ kick map for L-fucose bound to the $NADP^+$–L-fucose–BmulJ_04919 ternary complex. L-Fucose is shown as sticks with yellow, numbered carbons. (E) Stereoview of the interactions of L-fucose with BmulJ_04919. Protein atoms, L-fucose, and $NADP^+$ are shown as sticks with green, yellow, and white carbons, respectively.

stabilization of the α7–α8 loop in a conformation competent for binding L-fucose, followed by active site closure upon the formation of the numerous interactions with the substrate. On the basis of the number and specificity of the interactions, the structure of the ternary complex suggests that BmulJ_04919 would be fairly specific for L-fucose and that these binding determinants could be utilized to model the substrate specificity of homologues of BmulJ_04919.

DISCUSSION

Metal Content. LigI from *S. paucimobilis* was the first enzyme from cog3618 to be mechanistically and structurally characterized, and this enzyme does not require the binding of a divalent metal ion in the active site for catalytic activity.[7] BmulJ_04915, also a member of cog3618, shares ~20% identical sequence with LigI, and it is the second example of an enzyme within the AHS that does not require metal for catalytic function. We were unable to detect the binding of metals via ICP-MS in the samples of BmulJ_04915 purified in the absence of added metal, and thus, this protein does not require the metal for catalytic activity.

Active Site of BmulJ_04915. Nearly all members of the AHS are recognized by the conservation of five amino acid residues that form the active site and are utilized for metal binding and/or proton transfers. These residues include two histidine residues from the C-terminal end of β-strand 1, two additional histidine residues from the C-terminal ends of β-strands 5 and 6, and a conserved aspartate residue from the C-terminal end of β-strand 8.[5] In BmulJ_04915, three of the four histidine residues are conserved (His-9, His-11, and His-166) from the C-terminal ends of β-strands 1 and 6, in addition to the aspartate (Asp-244) from the end of β-strand 8. The histidine from the end of β-strand 5 is absent and replaced with Leu-141 (Figures 4B and 10A). In the absence of a metal ion bound in the active site, these four residues must now acquire new functional roles.

A structural alignment of the LigI and BmulJ_04915 active sites reveals relatively little conservation between the two binding pockets, aside from the residues predicted to confer catalytic activity (Figure 10A). A low level of conservation of the active site can be explained by analysis of the two significantly different substrates utilized by these enzymes. LigI catalyzes the hydrolysis of a planar dicarboxylated six-membered lactone, while BmulJ_04915 catalyzes the hydrolysis of a nonplanar six-membered lactone. The structure of BmulJ_04915 could not be obtained with bound substrate or product, but it is possible to manually dock the L-fucono-1,5-lactone substrate in the active site to obtain a view of the structural determinants for substrate binding (Figure 10B). Modeling L-fucono-1,5-lactone into the active site of BmulJ_04915 was based on the structural alignment with LigI (with bound product) and the general path of the bound HEPES molecule (Figures 4B and 10A). The sulfonate of the HEPES molecule bound to BmulJ_04915 is positioned like the newly formed carboxylate of the product of the reaction catalyzed by LigI (4-carboxy-2-hydroxymuconate) interacting with three histidine residues (His-9, His-11, and His-166), Arg-

dx.doi.org/10.1021/bi3015554 | *Biochemistry* 2013, 52, 239–253

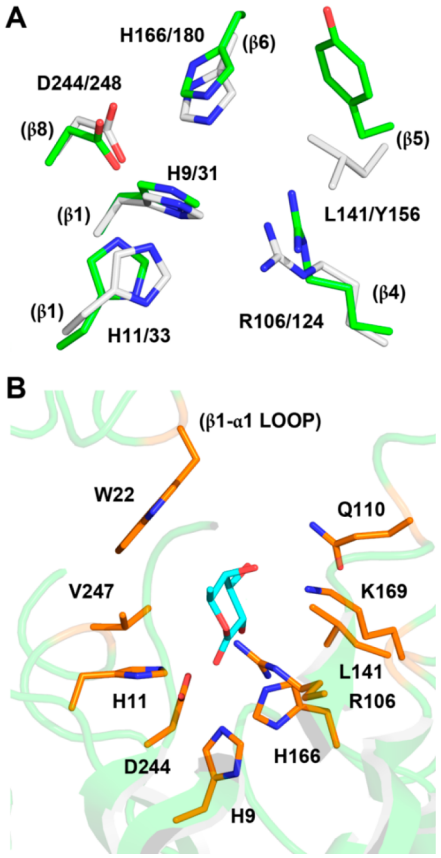

Figure 10. (A) Active site of BmulJ_04915 structurally aligned with that of 2-pyrone-4,6-dicarboxylic acid lactonase (LigI). The active site is color-coded as follows: green for LigI (PDB entry 4d8l) and white for BmulJ_04915. Numbers in parentheses designate the approximate locations in the secondary structure from which the residue originates. (B) L-Fucono-1,5-lactone modeled into the active site of BmulJ_04915.

106, and Asp-244 (Figure 4B). In this model, Gln-110 and Lys-169 are positioned to interact with hydroxyl groups at C-3 and C-4 of L-fucono-1,5-lactone. On either face of the lactone, Leu-141 and Leu-247 constrict the active site. Finally, Trp-22 lies against the aliphatic face of the lactone (C-3−C-4−C-5) near the entrance to the active site.

Proposed Mechanism of Action. The four AHS conserved residues (His-9, His-11, His-166, and Asp-244) align with their counterparts in LigI and assume similar roles in catalysis. The three conserved histidine residues polarize the carbonyl group of the sugar lactone substrate via electrostatic interactions.[7] The aspartate residue from β-strand 8 (Asp-244) is positioned to deprotonate an active site water molecule for nucleophilic attack on the C-1 carbonyl group of the lactone substrate. A fifth active site residue conserved within many members of cog3618 is an arginine from β-strand 4 (Arg-106). This arginine is proposed to assist in the cleavage of the lactone functional group through electrostatic interactions with the hydroxyl leaving group of the product. The proposed mechanism is presented in Scheme 3.

Natural Substrate of BmulJ_04915. BmulJ_04915 exhibits significant catalytic activity for a series of five-membered sugar lactones (Table 1) that share the same stereochemistry at C-2 and C-3 and has the highest activity for the L-fucono-1,4-lactone. The best substrate for BmulJ_04919 is β-L-fucose, which undergoes oxidation to L-fucono-1,5-lactone and subsequent nonenzymatic transformation to L-fucono-1,4-lactone. It has been postulated that the instability of D-galactono-1,5-lactone is due to an intermolecular rearrangement that occurs in a distorted chair conformation. The rearrangement is thought to arise from the axial hydroxyl group in C-4, which is positioned for nucleophilic attack on C-1.[38] A similar rearrangement is assumed for L-fucono-1,5-lactone and is fully consistent with the NMR data reported in this paper. The ^{1}H NMR spectra show a direct conversion of L-fucono-1,5-lactone to L-fucono-1,4-lactone without transformation to L-fuconate as an intermediate. The NMR spectra clearly show that BmulJ_04915 hydrolyzes L-fucono-1,5-lactone at a rate faster than that with L-fucono-1,4-lactone (Figure 6).

It was not possible to determine the kinetic constants for the hydrolysis of L-fucono-1,5-lactone because of chemical instability, and thus, a stable mimic was utilized. 4-Deoxy-L-fucono-1,5-lactone was synthesized enzymatically and provided a pyranosyl analogue that was more stable because of the absence of the axial hydroxyl group on C-4, which allowed the kinetic constants to be determined at pH 7.1. 4-Deoxy-L-fucono-1,5-lactone was shown to be hydrolyzed by BmulJ_04915 approximately 2 orders of magnitude faster than the corresponding L-fucono-1,4-lactone. Thus, even though L-fucono-1,5-lactone is kinetically unstable, it appears to be the natural substrate of BmulJ_04915.

The closest homologue (~27% identical sequence) of known function to BmulJ_04915 is SKA58_03595 from *Sphingomonas* sp. SKA58, which has been experimentally annotated as an L-rhamnono-1,4-lactonase.[9] Kinetic constants for L-rhamnono-1,4-lactonase have not apparently been reported, nor has a complete substrate profile been established. L-Rhamnono-1,4-

Scheme 3

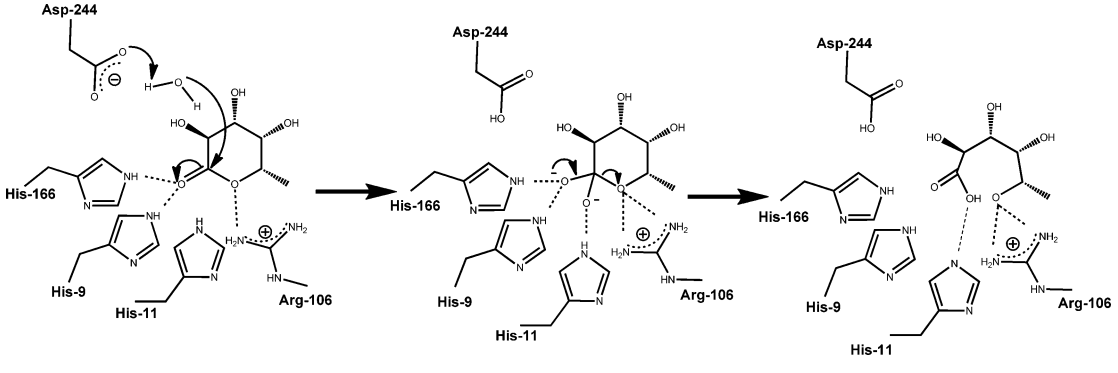

dx.doi.org/10.1021/bi3015554 | *Biochemistry* 2013, 52, 239−253

lactonase is adjacent to an L-rhamnose dehydrogenase from cog1028 that shares 30% sequence identity with BmulJ_04919. Given the sequence similarities, it is predicted that these homologues of BmulJ_04915 and BmulJ_04919 will act in a similar manner to produce a 1,5-lactone, which is subsequently hydrolyzed to the acid sugar.

Additional L-Fucono-1,5-lactonases. L-Fucono-1,5-lactonase activity was demonstrated in groups 1, 9, and 14 of cog3618 with enzymes Bamb_1224, Patl_0798, and BmulJ_04915, respectively (Figure 3 and Table 1). Groups 1, 9, and 14 are grouped together as part of Class I enzymes at a low-stringency E value of 10^{-30} and only begin to separate into more distinct groups at E values of $>10^{-70}$ (Figure 2B). A list of candidate L-fucono-1,5-lactonase sequences has been established. These proteins shared at least 30% sequence identity and map to the Class I enzymes in the sequence similarity network. All candidate sequences were aligned with the experimentally verified L-fucono-1,5-lactonase, BmulJ_04915. Sequences were considered to be L-fucono-1,5-lactonase if the following active site residues were conserved: His-9, His-11, Trp-22, Arg-106, Gln-110, His-166, Thr-207, Glu-208, and Asp-244. The 174 sequences that conform to the specific active site residues are now postulated to be L-fucono-1,5-lactonase proteins and are represented as yellow nodes in Figure 2 and are listed in Table S1 of the Supporting Information.

■ ASSOCIATED CONTENT

Supporting Information

Table S1 and Figure S1. This material is available free of charge via the Internet at http://pubs.acs.org.

Accession Codes

The X-ray coordinates of L-fucono-1,5-lactonase (BmulJ_04915) have been deposited in the Protein Data Bank as entries 4DLF, 4DLM, 4DO7, and 4DNM. X-ray coordinates for L-fucose dehydrogenase (BmulJ_04919) have been deposited as PDB entries 4GKB, 4GLO, and 4GVX.

■ AUTHOR INFORMATION

Corresponding Author

*F.M.R.: telephone, (979) 845-3373; fax, (979) 845-9452; e-mail, raushel@tamu.edu. S.C.A.: telephone, (718) 430-2746; fax, (718) 430-8565; e-mail, almo@aecom.yu.edu.

Funding

This work was supported in part by the Robert A. Welch Foundation (A-840) and the National Institutes of Health (GM 71790 and GM 93342).

Notes

The authors declare no competing financial interest.

■ ACKNOWLEDGMENTS

X-ray diffraction data for this study were measured at beamlines X29 of the National Synchrotron Light Source (NSLS), Brookhaven National Laboratory, and Lilly Research Laboratory Collaborative Access Team (LRL-CAT) at the Advanced Photon Source, Argonne National Laboratory. Use of the NSLS beamline is supported by Center for Synchrotron Biosciences Grant P30-EB-009998 from the National Institute of Biomedical Imaging and Bioengineering and by the U.S. Department of Energy, Office of Science, Office of Basic Energy Sciences, under Contract DE-AC02-98CH10886. Use of the Advanced Photon Source at Argonne National Laboratory was supported by the U.S. Department of Energy, Office of Science, Office of Basic Energy Sciences, under Contract DE-AC02-06CH11357. Use of the Lilly Research Laboratory Collaborative Access Team (LRL-CAT) beamline at Sector 31 of the Advanced Photon Source was provided by Eli Lilly Co., which operates the facility.

■ REFERENCES

(1) Becker, D. J., and Lowe, J. B. (2003) Fucose: Biosynthesis and biological function in mammals. *Glycobiology 13*, 41R−53R.

(2) Chan, J. Y., Nwokoro, N. A., and Schachter, H. (1979) L-Fucose metabolism in mammals. The conversion of L-fucose to two moles of L-lactate, of L-galactose to L-lactate and glycerate, and of D-arabinose to L-lactate and glycollate. *J. Biol. Chem. 254*, 7060−7068.

(3) Ghalambor, M. A., and Heath, E. C. (1962) The metabolism of L-Fucose. II. The enzymatic cleavage of L-fuculose 1-phosphate. *J. Biol. Chem. 237*, 2427−2433.

(4) Heath, E. C., and Ghalambor, M. A. (1962) The Metabolism of L-Fucose. I. The Purification and Properties of L-Fuculose Kinase. *J. Biol. Chem. 237*, 2423−2426.

(5) Seibert, C. M., and Raushel, F. M. (2005) Structural and Catalytic Diversity within the Amidohydrolase Superfamily. *Biochemistry 44*, 6383−6391.

(6) Tatusov, R. L., Natale, D. A., Garkavtsev, I. V., Tatusova, T. A., Shankavaram, U. T., Rao, B. S., Kiryutin, B., Galperin, M. Y., Fedorova, N. D., and Koonin, E. V. (2001) The COG Database: New Developments in Phylogenetic Classification of Proteins from Complete Genomes. *Nucleic Acids Res. 29*, 22−28.

(7) Hobbs, M. E., Malashkevich, V., Williams, H. J., Xu, C., Sauder, J. M., Burley, S. K., Almo, S. C., and Raushel, F. M. (2012) Structure and Catalytic Mechanism of LigI: Insight into the Amidohydrolase Enzymes of cog3618 and Lignin Degradation. *Biochemistry 51*, 3497−3507.

(8) Halak, S., Basta, T., Buerger, S., Contzen, M., Wray, V., Pieper, D. H., and Stolz, A. (2007) 4-Sulfomuconolactone hydrolases from *Hydrogenophaga intermedia* S1 and *Agrobacterium radiobacter* S2. *J. Bacteriol. 189*, 6998−7006.

(9) Watanabe, S., Saimura, M., and Makino, K. (2008) Eukaryotic and bacterial gene clusters related to an alternative pathway of nonphosphorylated L-rhamnose metabolism. *J. Biol. Chem. 283*, 20372−20382.

(10) Atkinson, H. J., Morris, J. H., Ferrin, T. E., and Babbitt, P. C. (2009) Using sequence similarity networks for visualization of relationships across diverse protein superfamilies. *PLoS One 4*, e4345.

(11) Yew, W. S., Fedorov, A. A., Fedorov, E. V., Rakus, J. F., Pierce, R. W., Almo, S. C., and Gerlt, J. A. (2006) Evolution of enzymatic activities in the enolase superfamily: L-Fuconate dehydratase from *Xanthomonas campestris*. *Biochemistry 45*, 14582−14597.

(12) Xiang, D. F., Kolb, P., Fedorov, A. A., Xu, C., Fedorov, E. V., Narindoshvili, T., Williams, H. J., Shoichet, B. K., Almo, S. C., and Raushel, F. M. (2012) Structure-based function discovery of an enzyme for the hydrolysis of phosphorylated sugar lactones. *Biochemistry 51*, 1762−1773.

(13) Aslanidis, C., and de Jong, P. J. (1990) Ligation-independent Cloning of PCR Products (LIC-PCR). *Nucleic Acids Res. 18*, 6069−6074.

(14) Studier, F. W. (2005) Protein production by auto-induction in high density shaking cultures. *Protein Expression Purif. 41*, 207−234.

(15) Fox, B. G., and Blommel, P. G. (2009) Autoinduction of protein expression. *Current Protocols in Protein Science*, Chapter 5, Unit 5, p 23, Wiley, New York.

(16) Tropea, J. E., Cherry, S., and Waugh, D. S. (2009) Expression and purification of soluble His(6)-tagged TEV protease. *Methods Mol. Biol. 498*, 297−307.

(17) Minor, W., Cymborowski, M., Otwinowski, Z., and Chruszcz, M. (2006) HKL-3000: The integration of data reduction and structure solution—from diffraction images to an initial model in minutes. *Acta Crystallogr. 62*, 859−866.

(18) Battye, T. G., Kontogiannis, L., Johnson, O., Powell, H. R., and Leslie, A. G. (2011) iMOSFLM: A new graphical interface for diffraction-image processing with MOSFLM. *Acta Crystallogr. 67*, 271−281.
(19) Evans, P. (2006) Scaling and assessment of data quality. *Acta Crystallogr. 62*, 72−82.
(20) Zwart, P. H., Afonine, P. V., Grosse-Kunstleve, R. W., Hung, L. W., Ioerger, T. R., McCoy, A. J., McKee, E., Moriarty, N. W., Read, R. J., Sacchettini, J. C., Sauter, N. K., Storoni, L. C., Terwilliger, T. C., and Adams, P. D. (2008) Automated structure solution with the PHENIX suite. *Methods Mol. Biol. 426*, 419−435.
(21) McCoy, A. J., Grosse-Kunstleve, R. W., Adams, P. D., Winn, M. D., Storoni, L. C., and Read, R. J. (2007) Phaser crystallographic software. *J. Appl. Crystallogr. 40*, 658−674.
(22) Lebedev, A. A., Vagin, A. A., and Murshudov, G. N. (2008) Model preparation in MOLREP and examples of model improvement using X-ray data. *Acta Crystallogr. 64*, 33−39.
(23) Arnold, K., Bordoli, L., Kopp, J., and Schwede, T. (2006) The SWISS-MODEL workspace: A web-based environment for protein structure homology modelling. *Bioinformatics 22*, 195−201.
(24) Koehn, R. K., Diehl, W. J., and Scott, T. M. (1988) The differential contribution by individual enzymes of glycolysis and protein catabolism to the relationship between heterozygosity and growth rate in the coot clam, *Mulinia lateralis*. *Genetics 118*, 121−130.
(25) Chapman, E., and Wong, C. H. (2002) A pH sensitive colorimetric assay for the high throughput screening of enzyme inhibitors and substrates: A case study using kinases. *Bioorg. Med. Chem. 10*, 551−555.
(26) Hall, R. S., Xiang, D. F., Xu, C., and Raushel, F. M. (2007) N-Acetyl-D-glucosamine-6-phosphate deacetylase: Substrate activation via a single divalent metal ion. *Biochemistry 46*, 7942−7952.
(27) Kamat, S. S., Bagaria, A., Kumaran, D., Hampton, G. P., Fan, H., Sali, A., Sauder, J. M., Burley, S. K., Lindahl, P. A., Swaminathan, S., and Raushel, F. M. (2011) Catalytic mechanism and three-dimensional structure of adenine deaminase. *Biochemistry 50*, 1917−1927.
(28) Smoot, M. E., Ono, K., Ruscheinski, J., Wang, P. L., and Ideker, T. (2011) Cytoscape 2.8: New features for data integration and network visualization. *Bioinformatics 27*, 431−432.
(29) Krissinel, E., and Henrick, K. (2004) Secondary-structure matching (SSM), a new tool for fast protein structure alignment in three dimensions. *Acta Crystallogr. 60*, 2256−2268.
(30) Sundlov, J. A., Garringer, J. A., Carney, J. M., Reger, A. S., Drake, E. J., Duax, W. L., and Gulick, A. M. (2006) Determination of the crystal structure of EntA, a 2,3-dihydro-2,3-dihydroxybenzoic acid dehydrogenase from *Escherichia coli*. *Acta Crystallogr. D62*, 734−740.
(31) Klasen, R., Bringer-Meyer, S., and Sahm, H. (1995) Biochemical characterization and sequence analysis of the gluconate:NADP 5-oxidoreductase gene from *Gluconobacter oxydans*. *J. Bacteriol. 177*, 2637−2643.
(32) Novotny, M. J., Reizer, J., Esch, F., and Saier, M. H., Jr. (1984) Purification and properties of D-mannitol-1-phosphate dehydrogenase and D-glucitol-6-phosphate dehydrogenase from *Escherichia coli*. *J. Bacteriol. 159*, 986−990.
(33) Yokochi, N., Nishimura, S., Yoshikane, Y., Ohnishi, K., and Yagi, T. (2006) Identification of a new tetrameric pyridoxal 4-dehydrogenase as the second enzyme in the degradation pathway for pyridoxine in a nitrogen-fixing symbiotic bacterium, *Mesorhizobium loti*. *Arch. Biochem. Biophys. 452*, 1−8.
(34) Schachter, H., Sarney, J., McGuire, E. J., and Roseman, S. (1969) Isolation of diphosphopyridine nucleotide-dependent L-fucose dehydrogenase from pork liver. *J. Biol. Chem. 244*, 4785−4792.
(35) Tsuji, Y., Koike, A., Yamamoto, K., and Tochikura, T. (1992) Purification and some properties of L-fucose dehydrogenase from *Agrobacterium radiobacter* and its application to the assay of bound-fucose in glycoconjugates. *Biochim. Biophys. Acta 1117*, 167−173.
(36) Yasutake, Y., Nishiya, Y., Tamura, N., and Tamura, T. (2007) Structural insights into unique substrate selectivity of *Thermoplasma acidophilum* D-aldohexose dehydrogenase. *J. Mol. Biol. 367*, 1034−1046.
(37) Lesk, A. M. (1995) NAD-binding domains of dehydrogenases. *Curr. Opin. Struct. Biol. 5*, 775−783.
(38) Ueberschar, K. H., Blachnitzky, E. O., and Kurz, G. (1974) Reaction Mechanism of D-Galactose Dehydrogenases from *Pseudomonas saccharophila* and *Pseudomonas fluorescens*. *Eur. J. Biochem. 48*, 389−405.